Supplement of

Evaluating High-Resolution Forecasts of Atmospheric CO and CO_2 from a Global Prediction System during KORUS-AQ Field Campaign

Wenfu Tang et al., 2017

1. Definition of Taylor score (Taylor, 2001)

$$S = \frac{4(1+R)^4}{(\hat{\sigma}_f+1/\hat{\sigma}_f)^2(1+R_0)^4} \qquad (S1)$$

where $\hat{\sigma}_f$ is the ratio of σ_f (standard deviation of the model) and σ_r (standard deviation of observations), R is correlation between model and observations, and R_0 is the maximum potentially realizable correlation (= 0.9 in this study).

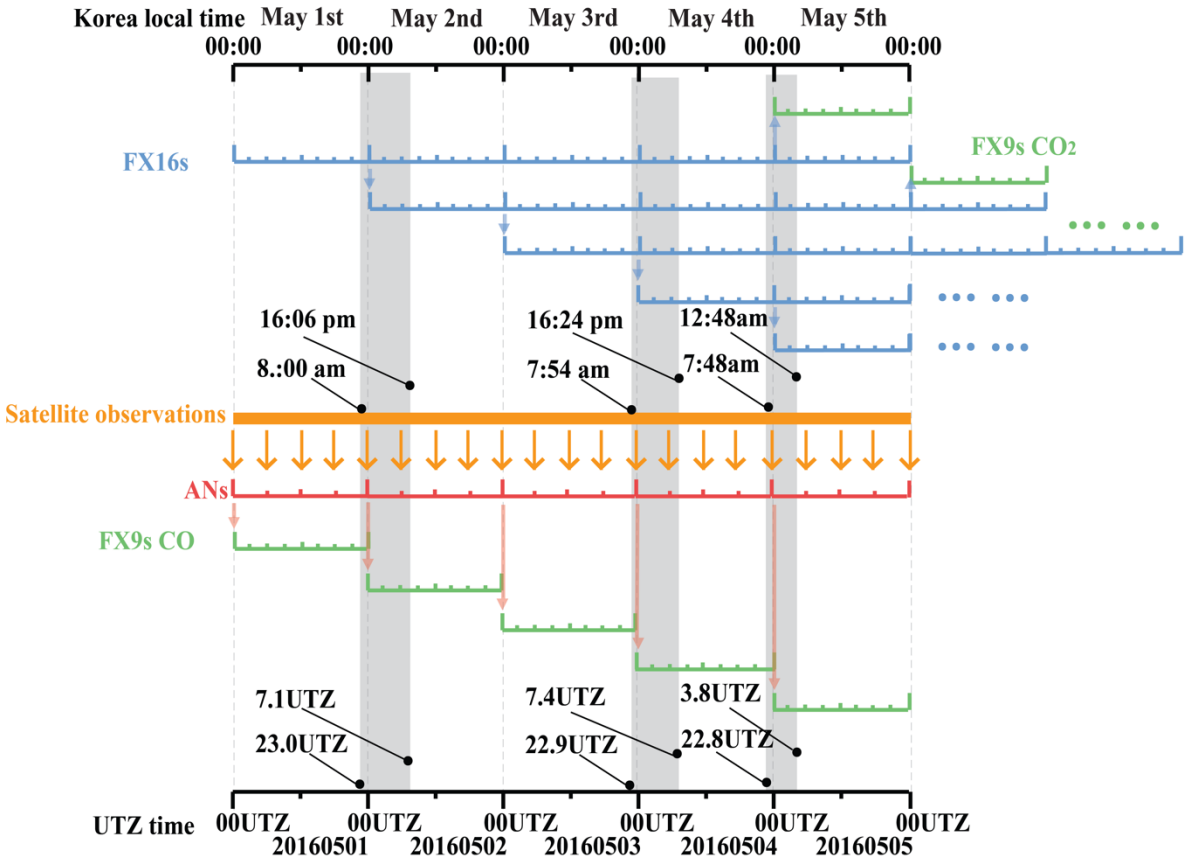

Figure S1. CAMS configuration. Left panel corresponds to the time configuration of the CAMS CO and CO2 evaluated in this study. The black lines represent Korea local time (on the top) and UTC time (on the bottom). The blue lines represent CAMS 5-day FC16s. FC16s are initialized with forecasts from the previous day. The orange line represents satellite observations (i.e., CO from MOPITT and IASI, CO2 from GOSAT) assimilated in CAMS (ANs). Gray shade denotes campaign time of the DC-8 aircraft. A typical DC-8 flight starts at 8am Korea time (23 UTC of previous day) and ends at 4pm Korea time (7 UTC).

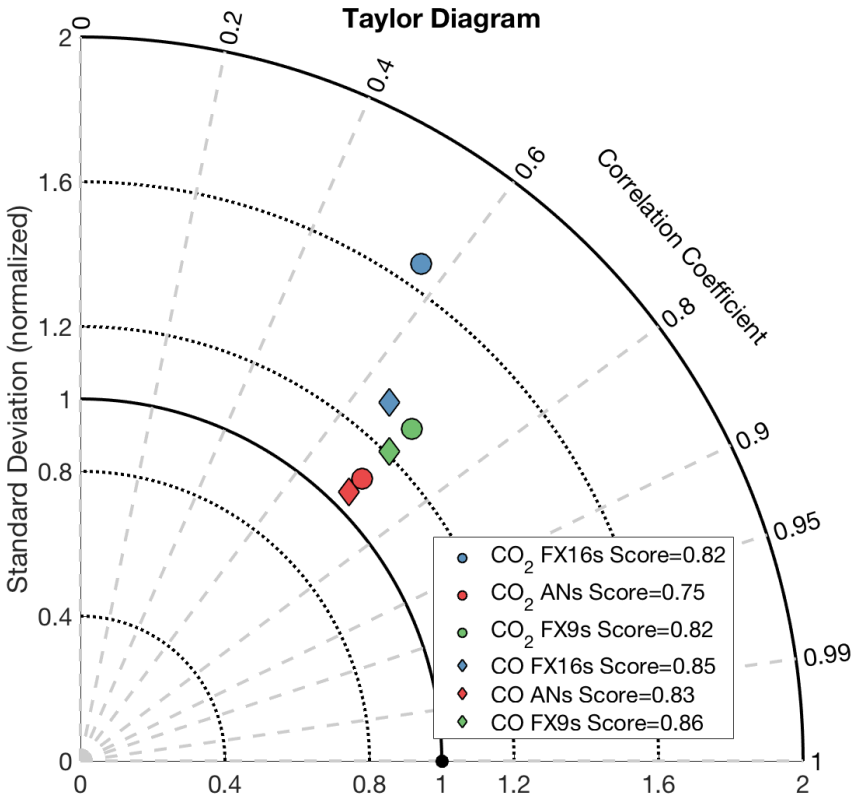

Figure S2. Taylor diagram for CAMS CO (diamonds) and CO_2 (circles) from FC9s (green), FC16s (blue), and ANs (red). Also shown are the Taylor scores.

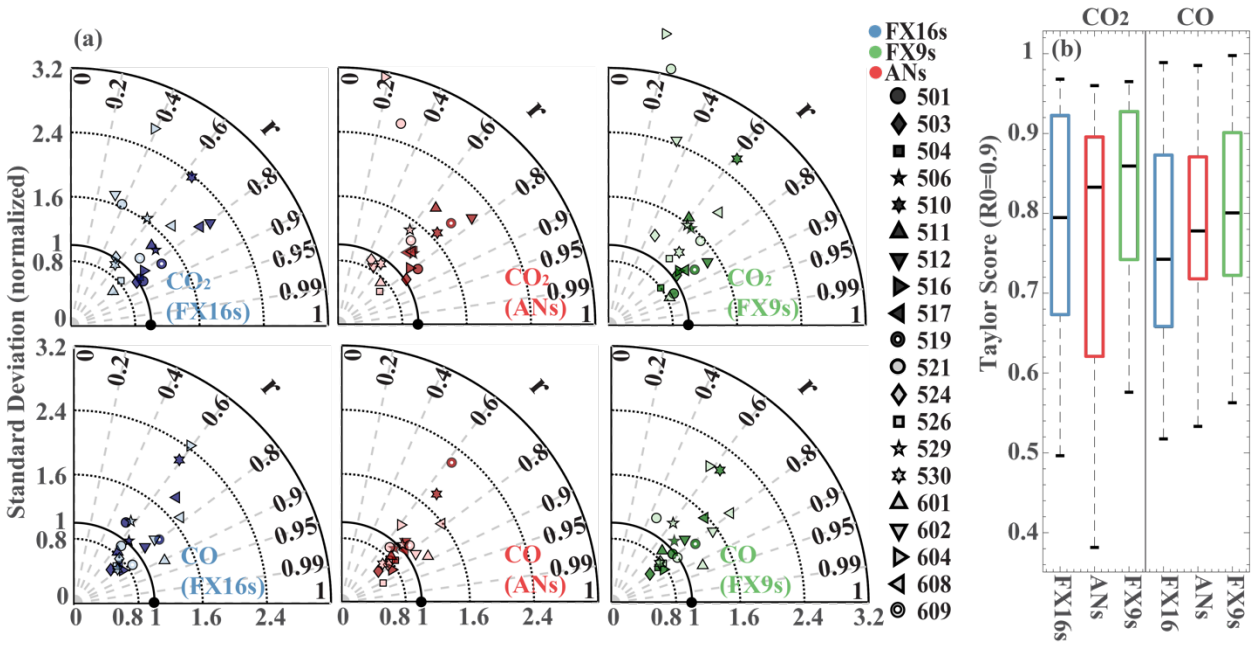

Figure S3. (a) Taylor diagrams for CAMS CO_2 (first row) and CO (second row) from 16-km forecasts (FC16s, left column), analyses (ANs, middle column), and 9-km forecasts (FC9s, right column) for individual flights (different symbols). (b) Boxplot of Taylor scores for CAMS CO_2 (left panel) and CO (right panel) from FC16s (blue), ANs (red), and FC9s (green).

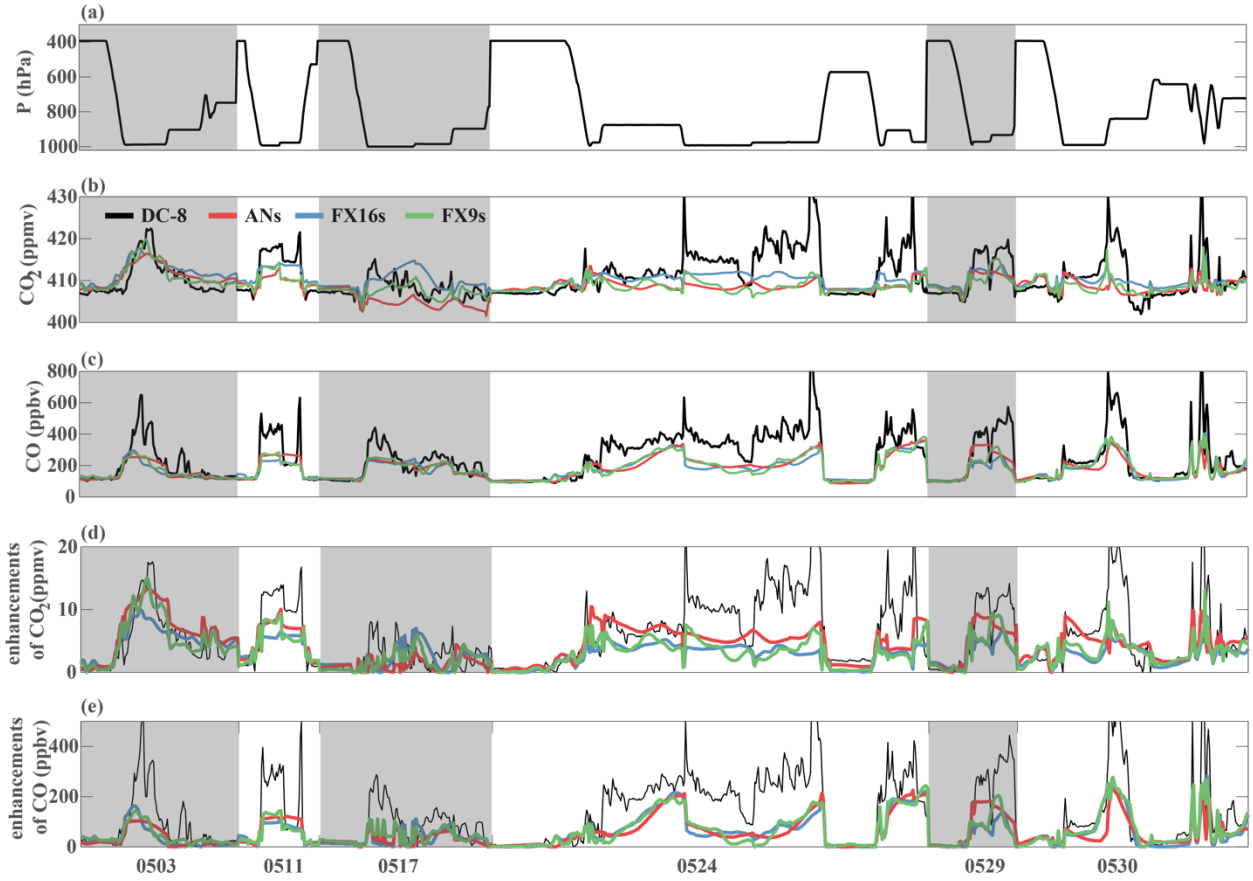

Figure S4. Time series of (a) pressure levels, (b) CO_2 concentrations and (d) their enhancements relative to background values, (c) CO concentrations and (e) their enhancements relative to background values along DC-8 aircraft tracks over the West Sea from measurements (black), 16-km forecasts (FC16s, blue), analyses (ANs, red), and 9-km forecasts (FC9s, green).

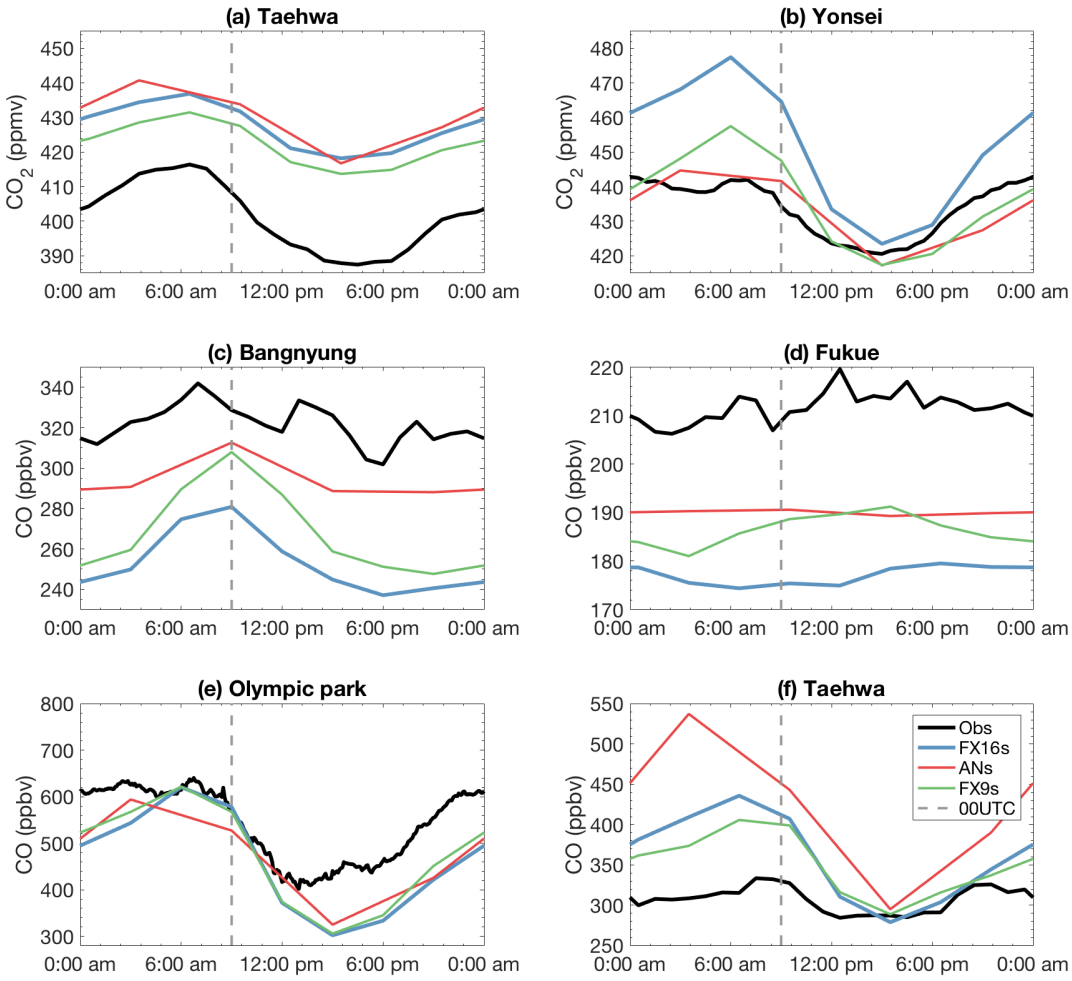

Figure S5. Diurnal cycles of CO_2 (a–b) and CO (c–f) concentrations averaged over days with available data during the KORUS-AQ period from observations (black), 16-km forecasts (FC16s, blue), analyses (ANs, red), and 9-km forecasts (FC9s, green) at fix ground sites, including (a, f) Taehwa, (b) Yonsei, (c) Bangnyung, (d) Fukue, and (e) Olympic park. CAMS values are averages across layers with pressure higher than 95% of the surface pressure.

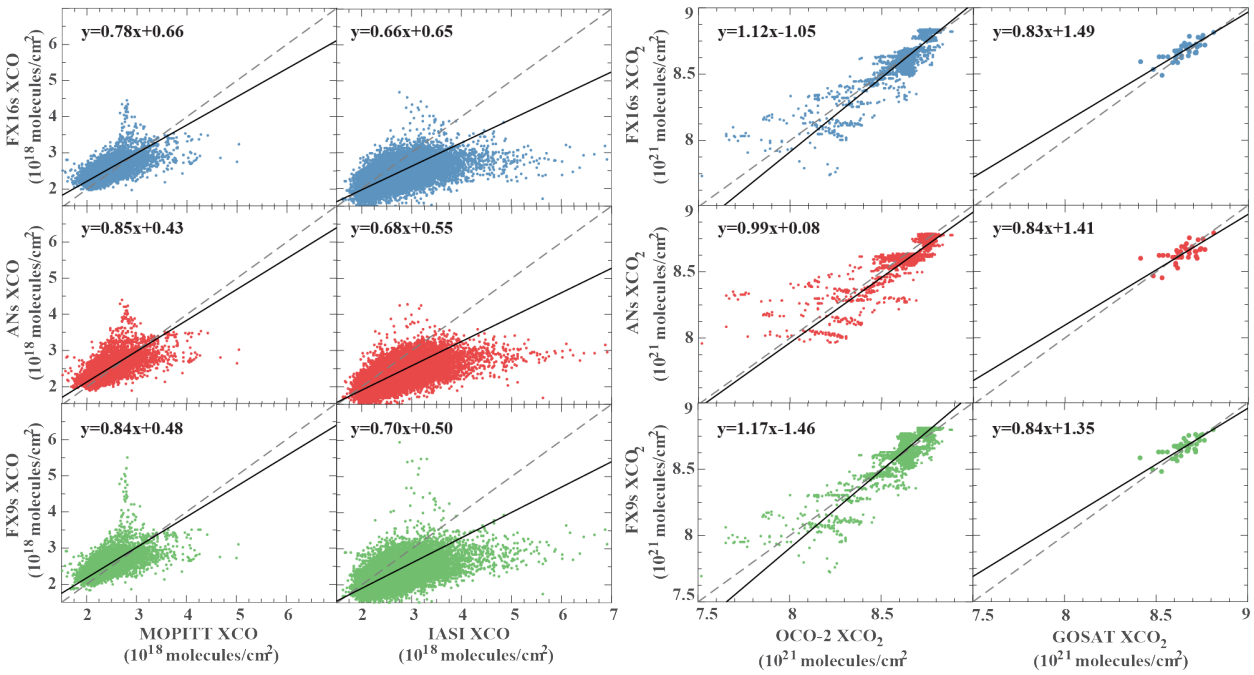

Figure S6. Comparisons between satellite observations and CAMS XCO and XCO2 from 16-km forecasts (FC16s, blue, 1st row), analyses (ANs, red, 2nd row), and 9-km forecasts (FC9s, green, 3rd row). The columns from left to right correspond to MOPITT XCO, IASI XCO, OCO-2 XCO2, and GOSAT XCO2, respectively.

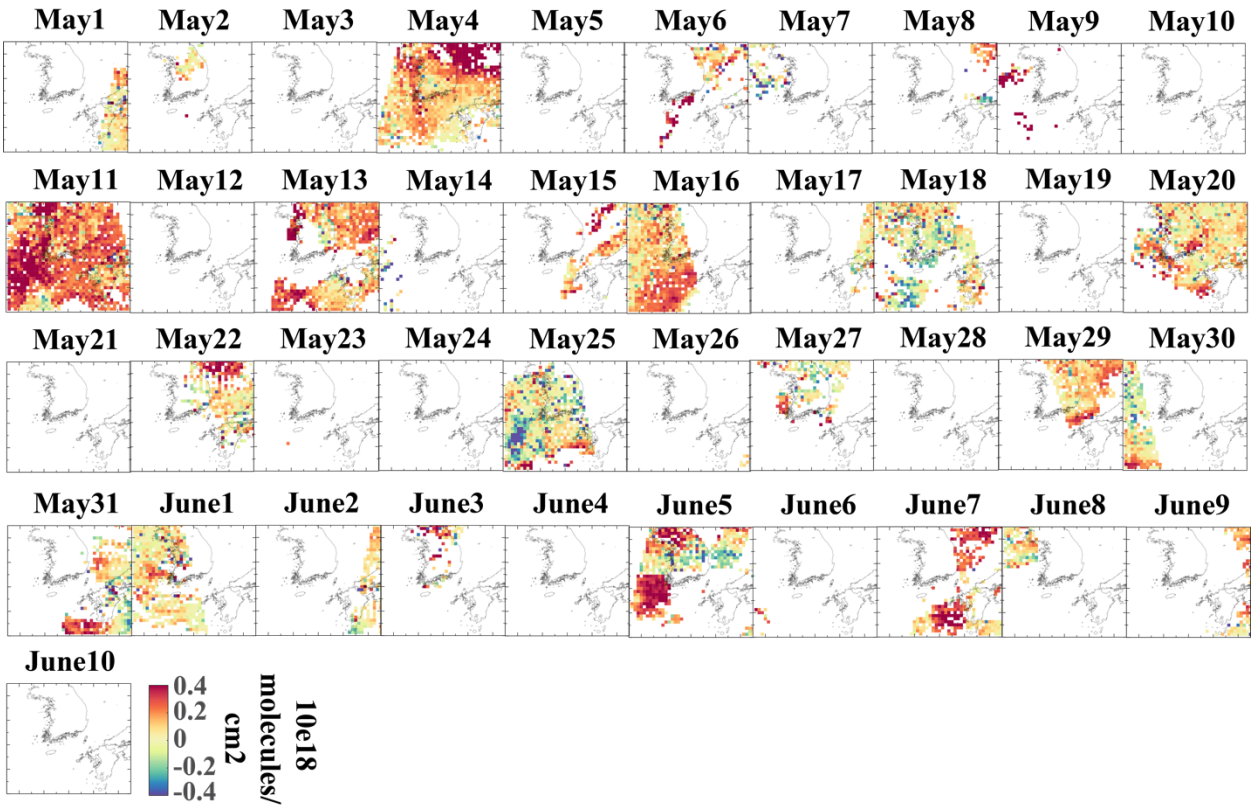

Figure S7. Daily spatial distributions of XCO biases in CAMS 9-km forecasts compared with MOPITT observations during the KORUS-AQ period (May 1 to June 10, 2016).